

# Earth and Space Science



## RESEARCH ARTICLE

10.1029/2023EA003403

# Modeling Temperature-Dependent Sub-Daily Extreme Rainfall With a Gridded Weather Generator

Jorge Sebastián Moraga<sup>1,2</sup> , Nadav Peleg<sup>3,4</sup> , and Paolo Burlando<sup>1</sup>

<sup>1</sup>Institute of Environmental Engineering, ETH Zürich, Zürich, Switzerland, <sup>2</sup>Fathom, Bristol, UK, <sup>3</sup>Institute of Earth Surface Dynamics, University of Lausanne, Lausanne, Switzerland, <sup>4</sup>Expertise Center for Climate Extremes, University of Lausanne, Lausanne, Switzerland

### Key Points:

- A new version of the AWE-GEN-2d weather generator model is presented
- The new model explicitly simulates the temperature dependency of extreme precipitation, enabling a realistic simulation of future extremes
- A climate change hydrological impact study over an alpine catchment is presented

### Supporting Information:

Supporting Information may be found in the online version of this article.

### Correspondence to:

J. S. Moraga,  
s.moraga@fathom.global

### Citation:

Moraga, J. S., Peleg, N., & Burlando, P. (2024). Modeling temperature-dependent sub-daily extreme rainfall with a gridded weather generator. *Earth and Space Science*, 11, e2023EA003403. <https://doi.org/10.1029/2023EA003403>

Received 3 NOV 2023

Accepted 25 MAY 2024

### Author Contributions:

**Conceptualization:** Jorge Sebastián Moraga, Nadav Peleg  
**Formal analysis:** Jorge Sebastián Moraga  
**Funding acquisition:** Paolo Burlando  
**Investigation:** Jorge Sebastián Moraga  
**Methodology:** Jorge Sebastián Moraga  
**Project administration:** Paolo Burlando  
**Software:** Jorge Sebastián Moraga, Nadav Peleg  
**Supervision:** Nadav Peleg, Paolo Burlando  
**Validation:** Jorge Sebastián Moraga  
**Writing – original draft:** Jorge Sebastián Moraga  
**Writing – review & editing:** Jorge Sebastián Moraga, Nadav Peleg, Paolo Burlando

**Abstract** Temperature increases are associated with an intensification of heavy sub-daily extreme rainfall by approximately 7% per °C, in accordance with the Clausius-Clapeyron (CC) relation. As a result of this intensification, there are concerns regarding the increased frequency and magnitude of floods in small to medium-sized catchments. The high-resolution two-dimensional weather generator (WG), AWE-GEN-2d, offers an ideal tool to simulate the climate variables required to assess the catchment-scale hydrological response at high resolution. However, it lacked an explicit representation of the relationship between temperature and precipitation that can mimic the CC relationship. Therefore, we introduce a newly revised version of the model, named AWE-GEN-2d-CC, designed to mirror the observed CC scaling by conditioning the simulation of precipitation properties (intensity and area) on temperature. We demonstrate the model's efficacy in representing future extreme rainfall by simulating their potential impact on the hydrological response of a mountainous catchment in the Swiss Alps. Based on observations and future climate model projections, AWE-GEN-2d-CC was used to generate large ensembles of present and end-of-century climate data at hourly and 2-km resolutions, used subsequently as input to Topkapi-ETH, a physically-based, distributed hydrological model. The new version of the WG successfully mimics the CC scaling of heavy rainfall, leading to an intensification of short-duration heavy rainfall in future climates, in contrast with the results obtained using the original model. This allows for a more realistic assessment of future rainfall impact on hydrological response, which, in the demonstration application, shows a modulated effect even for short durations.

**Plain Language Summary** As global temperatures continue to rise, so does the intensity of heavy rainfall, which can lead to increased flooding in small to medium-sized areas. The challenge is predicting not only how heavy rainfall will intensify at a specific point, but also how it is distributed over a catchment area. The AWE-GEN-2d model proved to be an effective tool in this respect. We introduce a new version of that model, called AWE-GEN-2d-CC, which explicitly considers the relationship between temperature and rainfall. We tested our model on a mountainous area in the Swiss Alps, using past observations and future climate model projections, and found that the model can successfully predict heavy rainfall intensification in the future, especially for short, intense bursts of rain. This improves the plausibility of the results compared to those obtained with the older version of the model. Despite the predicted increase in heavy rainfall, we found the effect on river flows in the catchment was less drastic. Our study highlights the importance of accurately modeling the impact of temperature on rainfall. In areas prone to high-intensity storms, our model can assist stakeholders in preparing for future weather extremes.

## 1. Introduction

Short, intense rainfall events have the potential to trigger pluvial floods, especially in small to medium-sized rural catchments (Wasko, Sharma, & Pui, 2021), as well as in mountainous (Moraga et al., 2021) and urban areas (O'Donnell & Thorne, 2020). The Clausius-Clapeyron (CC) relation, a well-established theory, postulates that the water-holding capacity of the atmosphere increases by ~7% for each °C increase in temperature (O'Gorman & Schneider, 2009; Trenberth et al., 2003). Consistent with this theory, numerous studies have shown that short-duration (daily to sub-daily) heavy rainfall intensities are indeed scaled with the temperature (Berg et al., 2013; E. M. Fischer & Knutti, 2016; Fowler et al., 2021; Marra et al., 2024; Molnar et al., 2015; Westra et al., 2014). While there have been reports of discrepancies, such as cases with no or negative scaling (Drobinski et al., 2016), it is now generally accepted that the scaling of short-duration rainfall intensity with temperature is indeed close to or above the theoretical CC-scale (Ali, Fowler, et al., 2021; Ali, Peleg, & Fowler, 2021).

© 2024. The Author(s).

This is an open access article under the terms of the [Creative Commons Attribution-NonCommercial-NoDerivs License](https://creativecommons.org/licenses/by/4.0/), which permits use and distribution in any medium, provided the original work is properly cited, the use is non-commercial and no modifications or adaptations are made.

Moreover, temperature appears to influence not only the rainfall intensity but also the area and temporal structure of the rainfall (Lochbihler et al., 2017, 2019; Peleg et al., 2018, 2022; Wasko et al., 2016).

General circulation models (GCMs) and regional climate models (RCMs) are frequently employed to project atmospheric changes, which result from varying greenhouse gas emission scenarios. However, the spatial resolution of these models, even that of the finer RCMs (with over  $10\text{ km} \times 10\text{ km}$  grid cells and daily time steps), is often too coarse to effectively resolve convective processes. Consequently, they depend on simplified parameterizations, leading to less reliable estimations of sub-daily extremes, and frequently missing the observed temperature-scaling evident in real-world observations (Ban et al., 2014; A. M. Fischer et al., 2015).

Alternatively, convection-permitting models (CPMs) are designed to explicitly resolve the convection at finer spatial resolutions ( $1\text{--}10\text{ km}^2$ ), which allows for realistic simulations of short-duration rainfall (Ban et al., 2021; Lucas-Picher et al., 2021; Pichelli et al., 2021; Prein et al., 2015, 2020; Vergara-Temprado et al., 2021). In fact, simulations by CPMs have shown that heavy short-duration rainfall, typically associated with events with intensities exceeding the 99th percentile (Fowler et al., 2021), often results from convection and that RCMs usually underestimate the rate of CC-scaling (Ban et al., 2018, 2021; Pichelli et al., 2021).

Furthermore, CPM simulations indicate that the rates of temperature-scaling are expected to persist under future global warming scenarios (Ban et al., 2018; Kendon et al., 2017; Pichelli et al., 2021; Vergara-Temprado et al., 2021). This underlines the importance of CPM projections for modeling the effects of climate change on short-duration heavy rainfall. The limitation of CPMs, however, lies in their high computational cost, which typically restricts their outputs to a single realization of a relatively short future climate simulation (Gutowski et al., 2020; Schär et al., 2020), limiting the possibility of conducting robust extreme value analysis or assessing projection uncertainties, such as those stemming from different emission scenarios or climate models (Addor et al., 2014; Fatichi et al., 2016; Moraga et al., 2022).

One potential solution to this challenge involves downscaling climate projections using stochastic weather generators (WG, Bordoy & Burlando, 2014; Fatichi et al., 2011; Fowler et al., 2007; Maraun et al., 2010; Peleg et al., 2019; Trzaska & Schnarr, 2014; Wilks & Wilby, 1999). Being relatively inexpensive in computational terms, WG are suitable to generate large ensembles of climate variables that are statistically similar to the observations used for calibration (Maraun et al., 2010; Wilks & Wilby, 1999). WGs can be re-parameterized using information from GCM/RCM to generate an ensemble of the future climate (e.g., Peleg et al., 2019). Moreover, by incorporating data from several climate models and multiple emission scenarios, WG can generate an ensemble that accounts not only for natural climate variability but also for the uncertainties emerging from climate models and emission scenarios (Fatichi et al., 2016; Moraga et al., 2022).

Numerous types of WGs exist, ranging from single-site (Fatichi et al., 2011) to multi-site (Sparks et al., 2018; Steinschneider et al., 2019; Verdin et al., 2018) to fully two-dimensional (Peleg et al., 2017; Singer et al., 2018), with the latter being the most suitable for characterizing highly heterogeneous climates. The AWE-GEN-2d model (Peleg et al., 2017) is a two-dimensional WG that can simulate the climate variables necessary for distributed hydrological modeling for both present and future climates at a high space-time resolution, as it is capable of simulations at sub-kilometer and sub-hourly scales (Peleg et al., 2019). Consequently, it has been employed for hydrological climate impact studies in many rural, urban, and mountainous catchments (Fatichi et al., 2021; A. M. Fischer et al., 2022; Moraga et al., 2021; Nyman et al., 2021; Peleg et al., 2020; Ramirez et al., 2022; Schirmer et al., 2022). However, one limitation of AWE-GEN-2d is its lack of explicit representation of the influence of temperature on rainfall fields, especially on heavy (convective) rainfall. This omission can lead to unrealistic scaling of storm properties with temperature, with disproportionate effects on short-duration rainfall. This limitation is particularly pronounced for future climate simulations, where the model relies on coarse-scale projections, which typically underestimate the intensity of convective storms.

Consequently, we introduce a new CC-scaling-capable version of the AWE-GEN-2d model, named AWE-GEN-2d-CC, which improves on the original model by Peleg et al. (2017) by explicitly conditioning rainfall properties to the near-surface air temperature at the onset of the event. We applied the new model version to a well-studied mountainous catchment in the Swiss Alps to demonstrate the effect that the new model has on the estimation of climate change impacts on streamflow by comparing the outputs obtained using the new and original models. Furthermore, we used the outputs of the WG to feed a physically-based, distributed hydrological model, Topkapi-

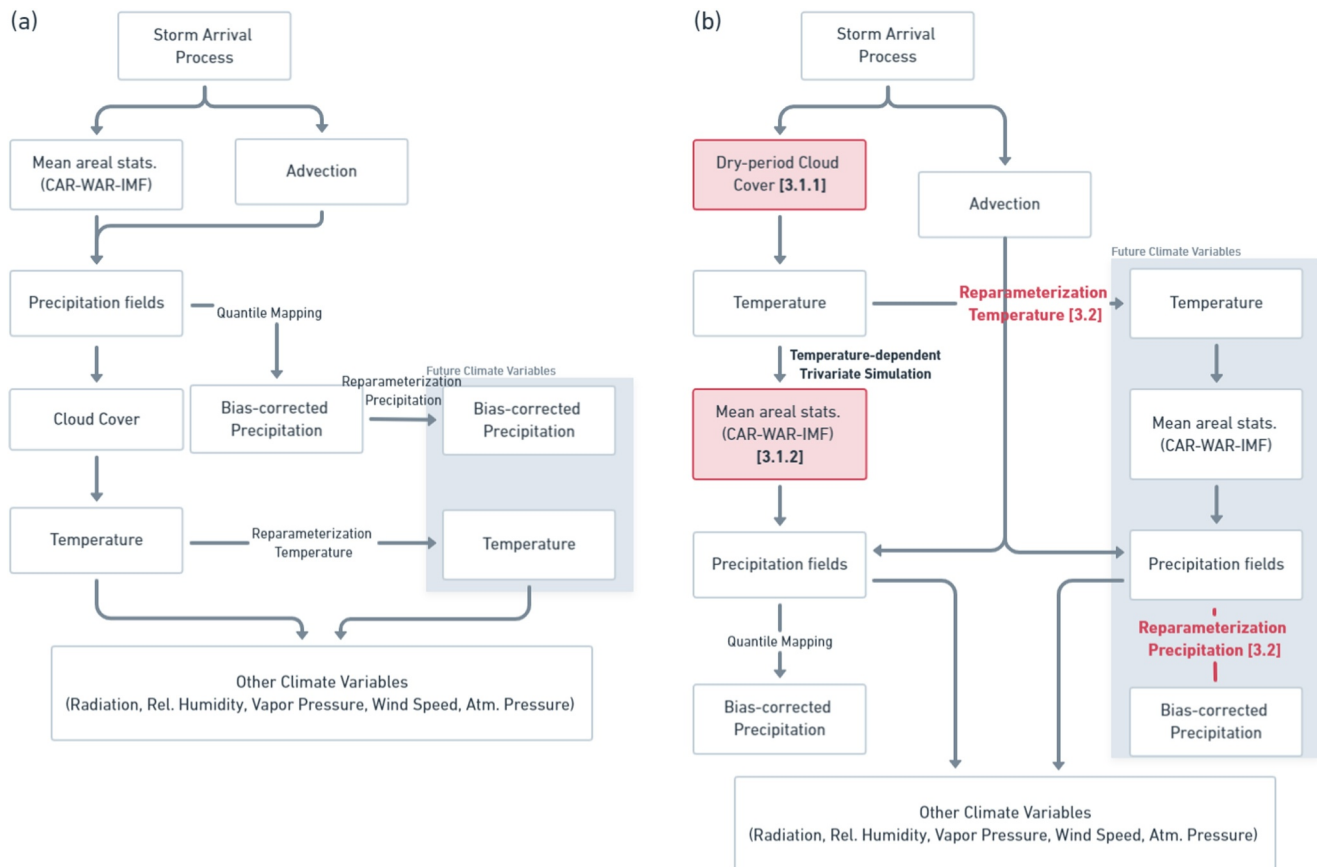


**Figure 1.** Flowchart describing the components of the two weather generators compared in this work. Panel (a) shows the structure of the original AWE-GEN-2d model (Peleg et al., 2017). Panel (b) shows the structure of the new version of the model here presented, AWE-GEN-2d-CC. The numbers in brackets indicate the section of this paper describing the corresponding procedure.

ETH (Fatichi et al., 2015), to assess the response of a mountainous catchment to extreme hydrometeorological events within the context of a warming climate.

## 2. The Original AWE-GEN-2d Model

The original AWE-GEN-2d model (Peleg et al., 2017) was designed to downscale coarse or sparse observational data into fine two-dimensional arrays of climate variables. It accomplishes this by combining physically-based equations with data-driven stochastic models which require observations from multiple sources, thus leveraging the capabilities of both stochastic and deterministic approaches. A thorough description of the model's structure is provided by Peleg et al. (2017), along with a Technical Reference in Supporting Information S2 detailing the equations that compose the different components of the model. In this section, we focus on a concise, qualitative overview of AWE-GEN-2d's modules (Figure 1a), aiming to facilitate the comparisons with our newly proposed model formulation (Figure 1b).

As illustrated in Figure 1a, AWE-GEN-2d operates in a sequence of interconnected modules. The simulation begins with the so-called storm arrival process, which determines the duration of alternating “wet” (indicating a precipitation event) and “dry” spells. For each precipitation event, the model simulates the joint temporal evolution of its mean areal statistics, that is, the wet area ratio (WAR), the mean precipitation over the domain (intensity mean field (IMF)), and the cloud cover area (CAR) at each time step. Notably, AWE-GEN-2d is built to preserve the auto- and cross-correlations among the three variables (Paschalis et al., 2013). For each dry spell, in turn, the model computes the evolution of CAR, which is influenced by the simulation of the preceding wet spell.

In parallel to the mean areal statistics module, the wind advection module simulates the velocity and direction of geostrophic winds as a stochastic process calibrated independently for wet and dry spells. Subsequently,

advection drives the movement of storm cells in the precipitation fields module. In this module, AWE-GEN-2d generates gridded precipitation that follows the temporal evolution of the mean areal statistics, as well as the spatial correlation and variability derived from remote sensing observations. Afterward, the model uses the precipitation fields to simulate the cloud cover evolution over every cell in the domain.

The temperature module in AWE-GEN-2d can be divided into two parts: first, the near-surface air temperature for a given reference elevation is computed as the sum of a deterministic and a stochastic component. The deterministic component depends on the previously simulated cloud cover, the incoming solar long-wave radiation at a given time, and the domain location and topology, whereas the stochastic component is modeled as an autoregressive process, calibrated based on ground observations. The second part of the module consists of computing near-surface air-temperature as the sum of the temperature at a reference elevation and a stochastic lapse-rate for each grid-cell, which allows the model to generate semi-continuous temperature fields over the domain.

Furthermore, the model generates the mean areal atmospheric pressure through an autoregressive model and then extends the calculations to the entire domain based on the simulated air temperature. The temperature is also used to calculate the vapor pressure, incoming shortwave radiation, relative humidity, and dew-point temperature; all of which are, in turn, dependent on each other and are therefore calculated iteratively. Lastly, the near-surface wind velocity is simulated based on cloud cover and storm advection.

Even from this brief description, it is apparent that AWE-GEN-2d is structured to preserve the observed cross-correlations between various climate variables. A conspicuous absence, however, is the influence of climate variables on the magnitude of precipitation intensities, which is our main motivation to develop the new AWE-GEN-2d-CC that is described next.

### 3. The AWE-GEN-2d-CC Model

Compared to its predecessor, the new formulation of the model presents a revised structure to include the dependency of heavy rainfall intensity and area on temperature. Consequently, the near-surface air temperature is now simulated before simulating the precipitation (Figure 1b). This generation sequence requires first simulating the cloud cover (i.e., CAR), as the temperature depends also on the shortwave radiation, which reaches the Earth is modulated by the effect of cloud cover. The CAR is simulated in two steps: first, the dry-spell cloud cover is simulated together with provisional values for the wet-spell cloud cover to simulate the temperature values; second, the final wet-spell CAR is simulated as part of a tri-variate process jointly with the area affected by precipitation WAR and the areal mean precipitation intensity IMF.

A flowchart illustrating the new model structure of AWE-GEN-2d-CC is shown in Figure 1b, whereas the description of the different modules is presented in the following sub-sections. Only the revised modules are presented and discussed as the rest of the model structure (i.e., the simulation of all other climate variables, besides precipitation, cloud cover, and temperature) is unchanged with respect to the original AWE-GEN-2d model. As in Peleg et al. (2017), the Supporting Information S2 of this manuscript contains the Technical Reference that provides the details about the formulations and equations of the new model.

#### 3.1. Cloud Cover

The new model structure requires the computation of cloud cover before the simulation of storm mean areal statistics, given that these are now dependent on the near-surface air temperature simulation and this, in turn, relies on the cloud cover. To reconcile this apparent paradox, the cloud cover for dry periods between storms ( $CAR_d$ ) and the cloud cover during storms ( $CAR_w$ ) are simulated by separate modules.

As in AWE-GEN-2d,  $CAR_d$  is modeled as a stochastic process where its mean value is a function of the distance to a storm occurrence and the stochastic component simulated as an autoregressive moving average model calibrated from observations. The novelty in the new structure is in the inclusion of an initial placeholder value for the cloud during wet events ( $CAR_w^*$ ), which can take the form of a trivial climatological estimation such as the mean during the observed record. The final  $CAR_w$  value replacing the placeholder value is subsequently simulated in the module that computes the mean areal statistics as one component of a tri-variate stochastic process along with the IMF and WAR variables.

### 3.2. Mean Areal Statistics

The temporal evolution of a storm is first described by three domain-averaged variables: (a) the fraction of the domain covered by clouds or wet-spell cloud area ratio ( $CAR_w$ ); (b) the fraction of the domain cells experiencing precipitation denoted as WAR; and (c) the mean areal intensity (IMF), which is the average of the precipitation (encompassing solid and liquid precipitation) over the entire domain at any given time. In AWE-GEN-2d-CC, as in its predecessor, the three variables are modeled jointly as part of a tri-variate stochastic process to preserve the observed auto- and cross-correlations of each field. The variables are simulated in the probability domain as a Gaussian stochastic process with a Whittle-Matérn class covariate function (Gneiting et al., 2010), which allows for taking advantage of the highly efficient Fast Fourier Transform method (Chambers, 1995; Frigo & Johnson, 1998) to obtain the correlated probabilities for the three variables. Finally, the probabilities are used to compute the real values of each areal statistic as the inverse of their corresponding marginal distribution.

In contrast with the previous model version, where seasonal parameter sets were used, the parameters that describe the Matérn covariate function (10 parameters), as well as the tri-variate Gaussian copula (7 parameters), are calibrated according to the average domain temperature at the onset of the precipitation event. Accordingly, as described in detail in Section 5.1 of the Technical Reference in Supporting Information S2, the time series of the three variables are transformed from the frequency to the real space using temperature-bin-dependent marginal distributions. By adapting the calibration and modeling to specific temperature ranges, this approach seeks to preserve the correlation of mean areal statistics with temperature as observed in real-world data, without assuming predefined temperature scaling rates of the marginal variables. This formulation ensures that the model captures the variable correlation between temperature and storm characteristics as empirically observed across different domains, rather than imposing a universal CC scaling rate.

### 3.3. Reparameterization Under Climate Change

To simulate future climate variables, Moraga et al. (2021, 2022) reparametrized AWE-GEN-2d following the blueprint laid out by Peleg et al. (2019). The procedure consists of using the so-called Factors of Change (FC) approach (see e.g., Bordoy & Burlando, 2014; Burlando & Rosso, 1991; Fatichi et al., 2011), which computes FCs from the outputs of present and future climate model simulations to alter the model parameters. For instance, the distributions for precipitation intensities are adjusted by combining a quantile mapping bias-correction method with the FC, thus ensuring that future precipitation simulations reflect the climate change signals.

To take advantage of the features introduced in AWE-GEN-2d-CC, it is key that the reparameterization preserves the observed scaling of storm properties with temperature, particularly regarding high precipitation extremes. For this reason, we adapted the approach presented by Peleg et al. (2019) to find an objective distribution function of the precipitation that fulfills two objectives: (a) aligning the location statistics (e.g., mean or median) with the FC, and (b) ensuring that the distribution's right-tail (as represented, e.g., by the variance or by a specific high quantile) corresponds to the changes simulated by the mean areal statistics module that results from the enforced temperature changes. The reparameterization algorithm can be accordingly summarized as follows:

- a. From GCMs/RCMs simulations, compute the FC of the location statistics of precipitation and temperature on a monthly or seasonal basis. For example, the FC for the mean of precipitation ( $FC_{\mu_p}$ ) is calculated as the ratio of the future ( $\mu_{Pr}^{RCM,fut}$ ) and present ( $\mu_{Pr}^{RCM,pres}$ ) means (Equation 1), whereas the FC of mean temperature ( $FC_{\mu_T}$ ) is calculated as the difference (Equation 2):

$$FC_{\mu_p} = \mu_{Pr}^{RCM,fut} / \mu_{Pr}^{RCM,pres} \quad (1)$$

$$FC_{\mu_T} = \mu_T^{RCM,fut} - \mu_T^{RCM,pres} \quad (2)$$

- b. Use the FC to modify the future temperature simulations in AWE-GEN-2d-CC, which in turn influences the simulation of future mean areal statistics.
- c. After executing the mean areal statistics module of AWE-GEN-2d-CC, compare the outputs of present and future IMF and use them to compute the FC for the precipitation right-tail statistics. For instance, the Factor of Change for the 99th quantile,  $FC_{q^{99},p_r}$ , is calculated in Equation 3:

$$FC_{q_{Pr}^{99}} = q_{Pr^{fut,sim}}^{99} / q_{Pr^{pres,sim}}^{99} \quad (3)$$

- d. At each domain grid cell find the parameters (location, shape, and scale) of the future precipitation distribution function  $F_x$  so that it most closely follows the observed statistics multiplied by the FCs computed in (a) and (c), such that:

$$\overline{F_x} \approx \mu_{Pr^{RCM,pres}} * FC_{\mu_{Pr}}, \text{ and} \quad (4)$$

$$F_x(q = 0.99) \approx q_{Pr^{pres,sim}}^{99} * FC_{q_{Pr}^{99}} \quad (5)$$

- e. Use quantile mapping, as shown by Peleg et al. (2019), to adjust the precipitation intensities simulated in the “Precipitation fields” module so that they follow the distribution found in (d).

Through this revised reparameterization approach, the model maintains the observed auto- and cross-correlations inferred under current climate conditions while, at the same time, it accommodates adjustments to climate-model-derived coarse-scale seasonal statistics.

## 4. Model Demonstration on a Case Study

### 4.1. Experiment Structure

The three objectives of the proposed demonstration experiment are: (a) to compare precipitation simulations between the original and new versions of the model and demonstrate that the new model structure reliably reproduces the observed climate while improving the simulation of extremes; (b) to evaluate the performance of AWE-GEN-2d-CC in reproducing the temperature dependence of storm properties in present and future climate simulations; and (c) to assess the effect of more realistic characterization of future precipitation extremes on the hydrological response of an exemplary mountainous catchment.

To accomplish the first two objectives, the numerical experiment was structured to generate a large number of simulations that allow for a robust analysis of extreme values. Concretely, a present-climate ensemble consisting of 900 years of simulations was generated based on the observed climate statistics representative of the 1976–2005 period. Likewise, we used the model to generate an ensemble of 900 years of future climate simulations following climate model projections for the end of the 21st century (period 2080–2089).

To address the third objective and measure the hydrological response under present and future climates, the 900 years of stochastic simulations generated for each climate scenario (present and future) were divided into 36 subsets of 25 years each. Each subset was used as input to the physically based, distributed hydrological Topkapi-ETH model (Fatichi et al., 2015), which is designed to reproduce a comprehensive set of hydrological processes, including the partition of liquid and solid precipitation, snow accumulation, redistribution, and melting, superficial runoff and channelized flow, evapotranspiration, infiltration and percolation of flow through lower soil layers, as well as soil and groundwater fluxes, among others. The resulting simulations, which characterize the present and end-of-century response of the catchment, enabled the analysis of the effects of climate change on hydrological statistics and their comparison with the results of a similar experiment carried out by Moraga et al. (2021, 2022), who used ensembles generated with the original AWE-GEN-2d model as inputs to Topkapi-ETH.

### 4.2. Study Area

The Kleine Emme is a mesoscale (478 km<sup>2</sup>) mountainous catchment located on the northern side of the central Swiss Alps. It has a complex topography, characterized by a relatively wide elevation range (from 438 to 2,330 m. a.s.l.) The mean annual precipitation over the catchment is around 1,650 mm and features heavy (convective) rainfall events during the warm season from May to September (Molnar et al., 2015). It has an average temperature of 7.6°C with January being the coldest month with an average of −1.1°C and July being the warmest

**Table 1**  
*Data Sources Used to Characterize the Kleine Emme Catchment*

Data	Source	Resolution
Digital elevation model	Swiss Federal Office of Topography (Swisstopo, 2002)	100 m × 100 m grid
Ground weather stations	SwissMetNet by MeteoSwiss (Table S1 in Supporting Information S1)	10-min
Weather radar	C-Band weather radar by MeteoSwiss (Germann et al., 2006)	2 km × 2 km grid, 5-min
Cloud cover	MERRA-2 reanalysis data set (Rienecker et al., 2011)	Hourly
Gridded precipitation	CombiPrecip by MeteoSwiss (Sideris et al., 2014)	2 km × 2 km grid, daily
Geostrophic wind velocity (500 hPa)	MERRA-2 reanalysis data set (Rienecker et al., 2011)	Hourly
Soil properties	Swiss Federal Office for Agriculture FOAG (Bundesamt für Statistik (BFS), 2020)	100 m × 100 m grid
Land cover types	Corine data set (“Corine Land Cover (CLC) map 2012,” 2014)	100 m × 100 m grid
Streamflow (Kleine Emme at Emmen)	Swiss Federal Office for the Environment (FOEN)	Hourly

month with an average of 16.2°C. The mean discharge at its outlet is 15.5 m<sup>3</sup> s<sup>-1</sup> (1,024 mm yr<sup>-1</sup>) with a maximum instantaneous observed peak of 650 m<sup>3</sup> s<sup>-1</sup> recorded in August 2005. In general, there are no major stream regulations, diversion, or abstractions, and most of the land cover is either natural pasture or crops, with little presence of urbanized areas. The location, elevation map, and elevation distribution are shown in Figure S1 in Supporting Information S1.

### 4.3. Data

The data used in this experiment was retrieved from multiple publicly available data sources including geographical information, weather stations, remote sensing, and reanalysis data sets. To set up the two versions of the WG model (the same data was used for both versions), the domain's topography was described by a high-resolution digital elevation model (DEM, Swisstopo, 2002). Weather radar observations were used to extract information regarding the storm-arrival process as well as the spatiotemporal structure of storms. This was complemented by ground temperature measurements used to determine the temperature at the onset of events and model the temperature lapse rate over the domain. Cloud cover data and advection velocities were modeled to follow the MERRA-2 reanalysis data set (Rienecker et al., 2011). Finally, the gridded, hourly precipitation reanalysis data set CombiPrecip (Sideris et al., 2014), produced by the Swiss meteorological office MeteoSwiss, is used as a reference to correct the bias in simulated AWE-GEN-2d-CC outputs.

The domain for the Topkapi-ETH simulations was characterized using the aforementioned DEM, as well as soil types and land cover maps (see Table 1) to assign hydraulic soil properties, soil depth, evapotranspiration parameters, and surface roughness values to each grid cell. The streamflow data to perform the calibration of the model, described in Moraga et al. (2021), was obtained from hourly records at the outlet of the catchment located in the locality of Emmen, Lucerne, provided by the Swiss Federal Office for the Environment. A summary of the data used in this study is provided in Table 1.

### 4.4. Extreme Value Analysis

The frequency and magnitude of extreme hydrometeorological events were quantified using the Generalized Extreme Values distribution (GEV, Jenkinson, 1955). First, the simulations of climate and hydrological data were divided into 36 realizations of 25-year durations. For each realization, the yearly block maxima were fitted to the GEV distribution, from which the return periods of each considered variable were extracted. Lastly, the interquartile ranges (IQR) of the return periods of the (36) realizations were calculated to quantify the variability of the outputs.

### 4.5. Calibration

The calibration procedure of AWE-GEN-2d for the Kleine Emme catchment is presented in detail by Moraga et al. (2021) and will not be addressed in this text. Instead, this section will focus on the calibration aspects relevant to the changes introduced with the new model structure of AWE-GEN-2d-CC, that is, the cloud cover and storm properties simulations (see Sections 3.1 and 3.2). A detailed account of the calibration methodology,

encompassing the equations underpinning all the modules of AWE-GEN-2d-CC, can be found in the Technical Reference included in Supporting Information S2.

The hourly time series of CAR reanalysis data was divided into months and into wet and dry spells based on weather radar observations of precipitation used to determine the occurrence of wet or dry spells. The calibration of the dry-spell cloud cover,  $CAR_d$  was split into a deterministic and a stochastic component: First, the mean of its deterministic component was assumed to follow a two-term exponential function of the distance from the closest wet period, whereas the standard deviation is modeled simply as the average of all observations (Table S3 in Supporting Information S1). Subsequently, the stochastic component was modeled as an autoregressive moving-average process of the  $CAR_d$  time series (Table S4 in Supporting Information S1), previously normalized by fitting them to a Johnson-SB distribution as shown in Figure S2 in Supporting Information S1. In turn, the placeholder wet-spell cloud cover  $CAR_w^*$  values were obtained as a constant monthly value equal to the average cloud cover during wet events (Table S5 in Supporting Information S1).

Unlike the monthly-calibrated dry-spell cloud cover, the statistics of cloud and precipitation during storms are calibrated based on the temperature during a wet spell. To this effect, we split the record of event-averaged  $CAR_w$ , WAR, and IMF into temperature bins based on the domain-averaged temperature at the onset of a wet period (similar concept as presented by Ali, Fowler, et al., 2021; Ali, Peleg, & Fowler, 2021). We defined a total of 8 temperature bins with a width of 3°C for the six intermediate ones and an infinite width for the extremes (Figure S3 in Supporting Information S1). This configuration allowed us to balance a sufficient number of samples in each bin with a smooth transition of the temperatures in the 5–25°C range where, as shown in Figure S4 in Supporting Information S1, we observe a strong correlation between extreme precipitation and temperature.

For each temperature bin, we normalized the subset of event-averaged  $CAR_w$ , WAR, and IMF and computed their auto- and cross-correlation coefficients (Table S6 in Supporting Information S1), which are used as parameters to the Whittle-Matérn function used to model the covariate of the tri-variate probabilities. Subsequently, we used the mean and standard deviations of the normalized  $CAR_w$ , WAR, and IMF sequence to fit the seven-dimensional copula of the Gaussian process that describes their joint temporal evolution.

To simulate future climate statistics as outlined in Section 3.3, we obtained  $FC_{\mu_{Pr}}$  and  $FC_{\mu_T}$  (Table S7 in Supporting Information S1) from the outputs of nine GCM-RCM model chains (Table S2 in Supporting Information S1) developed under the EURO-CORDEX initiative (Jacob et al., 2014; Kotlarski et al., 2014) and later post-processed by MeteoSwiss (CH2018, 2019). The model's simulated temperature was adjusted by adding the monthly  $FC_{\mu_T}$  to the simulated time series. Subsequently, after simulating the future precipitation (conditioned by future temperatures) we computed the 99th quantiles of hourly precipitation for the present and future simulations to obtain  $FC_{q^{99}_{Pr}}$  (Table S2 in Supporting Information S1). We parameterized the distributions of present-climate precipitation by fitting the hourly time series of each grid cell to either a Generalized Pareto (GP) or Gamma distributions based on a typical goodness of fit criterion. Then, the GP or Gamma distributions of future precipitation were obtained by optimizing the fit to the objective monthly means (Equation 4) and 99th quantiles (Equation 5), and were used to correct the future precipitation intensities using quantile mapping.

As for the hydrological model employed in this experiment, we made no changes to the configuration of TOPKAPI-ETH used to model the response of the Kleine Emme in the previous work of Moraga et al. (2021), where the authors describe the calibration and validation procedures.

#### 4.6. Validation

We tested AWE-GEN-2d-CC's capacity to reproduce plausible climate variables by comparing the statistics of the simulated ensembles with those of observed data sets that were not directly used in the calibration, as well as with the outputs of AWE-GEN-2d simulations. Here, we focus on the validation of the novel aspects of AWE-GEN-2d-CC relative to its predecessor, namely, the change in the modeling of cloud cover, the effect that it has on temperature, especially during wet periods, and the new temperature-dependent simulation of areal storm properties. As for the remaining modules, their calibration and validation have been presented in a previous work (Moraga et al., 2021, 2022) and remain unaffected by the new model formulation. Conversely, although the calibration of the Topkapi-ETH hydrological model for Kleine Emme has also been addressed in the cited experiments, the newly generated climate data prompts us to revisit how the catchment responds to present-climate inputs, which we do in Section 4.6.4.

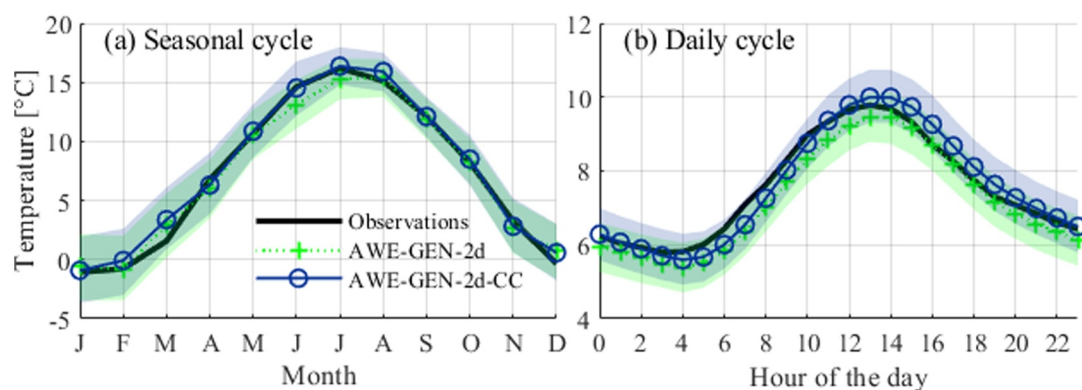


**Figure 2.** The two panels show the seasonal (a) and daily (b) cycles of near-surface air temperature as computed from the observations (solid black line), the AWE-GEN-2d simulations (dotted green line) and the new AWE-GEN-2d-CC simulations (solid blue line). The shaded areas depict the 5th–95th quantile range of the simulation ensembles.

#### 4.6.1. Cloud Cover

Although the simulation of cloud cover is executed by the same procedure as that used in AWE-GEN-2d, the new structure of AWE-GEN-2d-CC simulating the dry-period  $CAR_d$  before the wet-period  $CAR_w$ , implies that it is not possible to ensure smooth transitions between wet and dry periods in the  $CAR$  time series, as illustrated, for instance, in Figure S5 in Supporting Information S1. However, this effect is relatively minor and does not impact the overall  $CAR$  distribution. Figure S6 in Supporting Information S1 compares the observed and simulated  $CAR$  monthly distributions for the dry periods using both model versions. We find that AWE-GEN-2d-CC simulations underestimate the frequency of very low ( $<0.1$ ) and very high ( $>0.9$ ) cloud cover values at similar rates to AWE-GEN-2d (e.g., the proportion of very high values is 1.8% less than in the observations). Nonetheless, this new way of calculating the  $CAR$  allows for a satisfactory computation of the near-surface air temperature, as is shown in Section 4.6.2.

#### 4.6.2. Temperature

The calibration and simulation of temperature in AWE-GEN-2d-CC are performed as in its predecessor and therefore exhibit a good performance in resembling the observed seasonality, daily cycle, and spatial distribution, as shown in Figure 2. For instance, the root mean squared error of the monthly areal averages is  $0.7^\circ\text{C}$  ( $0.77^\circ\text{C}$  when using AWE-GEN-2d) and  $0.29^\circ\text{C}$  ( $0.40^\circ\text{C}$ ) for the average hourly daily cycle. A remaining concern has to do with the effect of using a placeholder value of cloud cover,  $CAR_w^*$ , in the modeling of temperature. As shown in Figure S7 in Supporting Information S1, which depicts the monthly distributions of temperature during wet events, the new model formulation behaves similarly to the previous model, hence we conclude that the use of the placeholder  $CAR_w^*$  does not have a noticeable impact on the temperature simulations.

#### 4.6.3. Precipitation

The main novelty of AWE-GEN-2d-CC is the temperature-dependent parameterization of storm properties, which aims to preserve the observed temperature scaling of intense precipitation. Consequently, we verify that change in the model structure does not affect the model performance in reproducing the storm properties under present climate conditions, and that these are as well characterized as by the previous model version. Indeed, as the boxplots plots of the event-averaged IMF and WAR in Figure 3 show, the statistics coming from the new AWE-GEN-2d-CC (e.g., WAR median of 0.34, IMF median of  $0.43 \text{ mm hr}^{-1}$ ) match those coming from the CombiPrecip ( $0.30$  and  $0.40 \text{ mm hr}^{-1}$ , respectively) reanalysis even better than the previous model version ( $0.57$  and  $0.32 \text{ mm hr}^{-1}$ ). Furthermore, the monthly distribution of the simulated hourly IMF time series, shown in Figure S8 in Supporting Information S1, matches the results using the previous model version. A closer look at the extreme IMF values is shown in the q-q plots of Figure S9 in Supporting Information S1, where it is evident that the WG underestimates the highest IMF quantiles, especially during the colder months (e.g., 24% in February, 21% in November). Moreover, the model successfully reproduces the seasonality of precipitation, as shown in Figure 4, with minor underestimations of up to 9% (January), well within the IQR of simulated outcomes. When

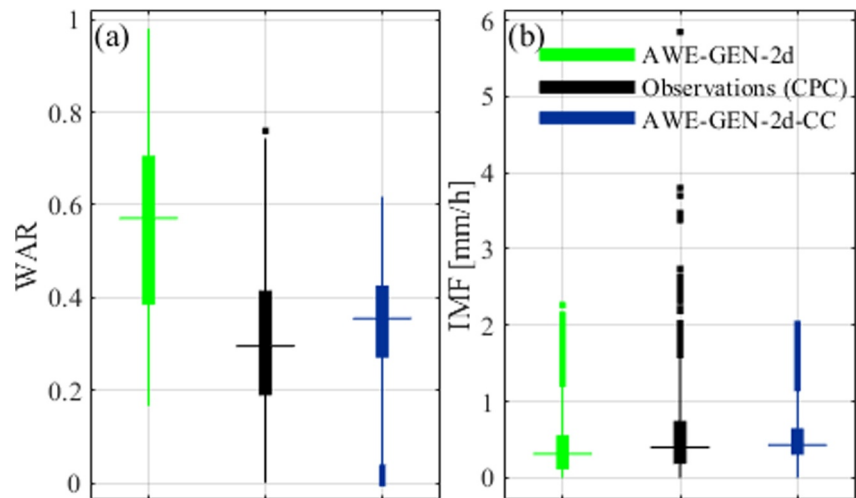


**Figure 3.** Boxplots of event-averaged wet area ratio (WAR) (a) and intensity mean field (b) as obtained from hourly records of CombiPrecip (black, middle) and simulations using AWE-GEN-2d (green, left), and the new AWE-GEN-2d-CC (red, right). Note that we only considered events with WAR over 0.1.

compared against the three long-standing weather stations in the domain (Figure S10 in Supporting Information S1), the model matches satisfactorily the monthly precipitation for the Luzern station located in the valley but struggles to match the statistics of the stations Napf and Pilatus, which are located in mountain tops. This is likely due to discrepancies between the CombiPrecip interpolated data set, which has been used for the WG calibration and validation, and the ground observations. In turn, the spatial distribution of precipitation shows an excellent agreement with errors below 3% of annual precipitation, as shown in Figure 5.

#### 4.6.4. Hydrological Response

To assess the influence of accounting for CC-scaling in future climate as simulated by the new model on the catchment response, the generated data was used as input to Topkapi-ETH, for which we used the same parameterization adopted by Moraga et al. (2021). As shown in Figure 6, the flow duration curve corresponding to this experiment matches the shape of that corresponding to the use of AWE-GEN-2d but has a lower magnitude across the entire domain of exceedance probabilities. The average underestimation is on average 12% and is more pronounced for lower exceedance probabilities. While this variation falls within the uncertainty range of model simulations (depicted as dashed lines in the figure), it is primarily attributable to the overall lower rainfall amounts simulated by the new WG compared to its predecessor. Regardless of the differences between the two

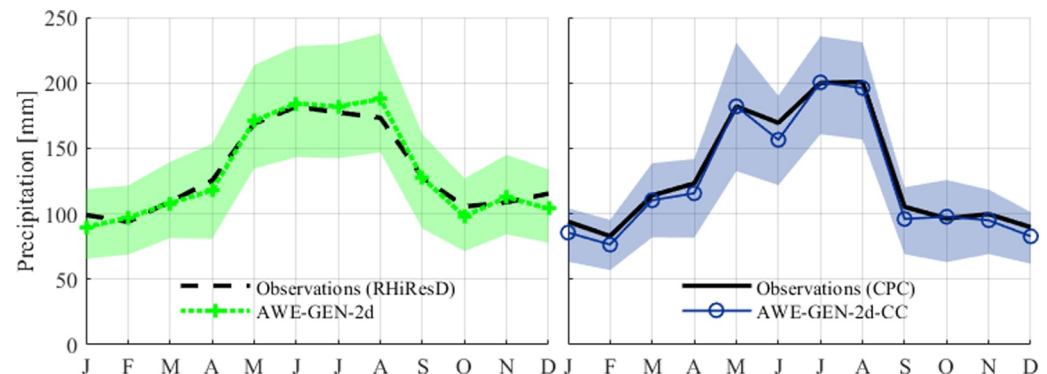


**Figure 4.** Comparison of the simulated and observed mean monthly precipitation using the AWE-GEN-2d model (left panel) and the new AWE-GEN-2d-CC model (right panel), with the interquartile range of the simulated outputs shown as shaded area. Each model is compared against the respective precipitation data set used for correcting the bias of the simulated outputs: CombiPrecip (Sideris et al., 2014) for AWE-GEN-2D-CC and RHiresD (MeteoSwiss, 2016) for AWE-GEN-2d in the study by Moraga et al. (2021, 2022).

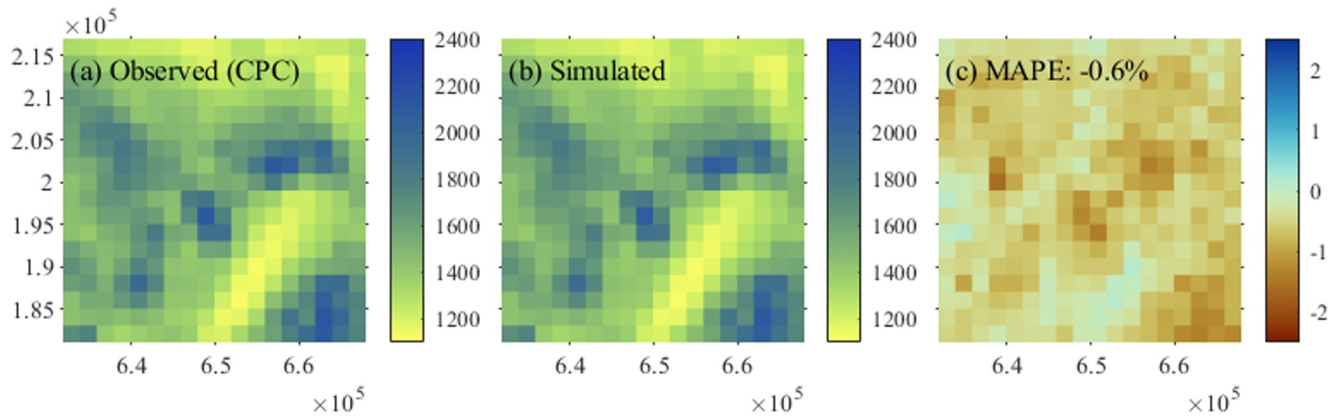


**Figure 5.** Mean annual precipitation (in mm) over the Kleine Emme domain according to CombiPrecip reanalysis data (a), present-climate AWE-GEN-2d-CC simulations (b), and mean absolute percentual error of the simulations (c). The coordinates are shown in meters using the UTM 32N projection.

experiments, the statistics of low exceedance streamflow (representing higher flows) align in both cases closely with the observations, while lower flows tend to be overestimated.

## 4.7. Results

### 4.7.1. Impacts on Precipitation

As shown in Figure 7a, the monthly mean areal precipitation follows the overall signal of the GCM-RCM climate trajectories projecting a slight average decrease in precipitation (−3.9%), which is concentrated in the summer months. The changes are spatially heterogeneous, with projected increases in the northeast part of the catchment of up to 14% and decreases in other areas of up to −11% (Figure 7b).

The newly formulated AWE-GEN-2d-CC model successfully emulates the scaling relationship between high precipitation intensities (above the 99th percentile) and temperature for the historical climate. Consequently, this capability is effective also in future climate simulations, as can be noted by the quantile regressions shown in Figure 8. Although the scaling slope is less pronounced compared to that computed from the observed data (e.g., slopes of 5.4% and 5.5% for the 0.99 quantile regression compared to an observed 6.0%, as shown in Figure S4 in Supporting Information S1), the impact of accounting for temperature-precipitation dependence is discernible

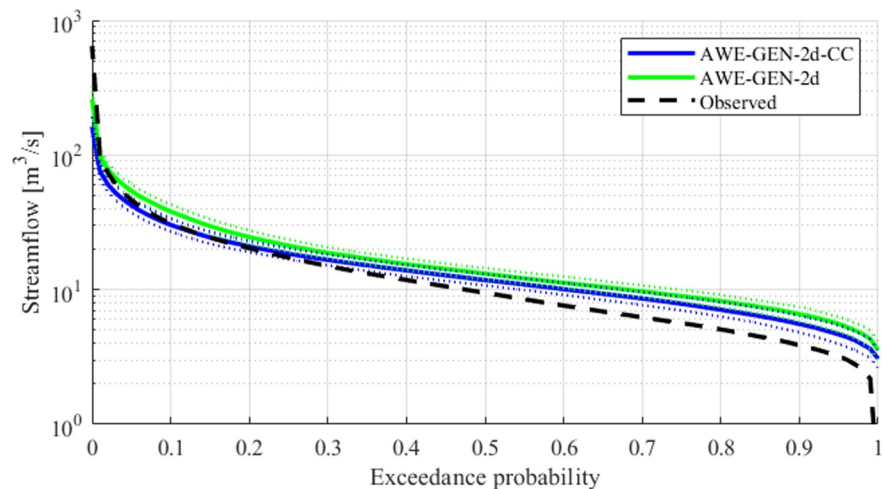


**Figure 6.** Duration curves for the observed streamflow record (black dashed line) and the ensembles of present-climate simulations using Topkapi-ETH. Input data was generated with AWE-GEN-2d (green) and AWE-GEN-2d-CC (blue). The solid lines represent the median across realizations and the dashed lines indicate the interquartile range for each exceedance probability.

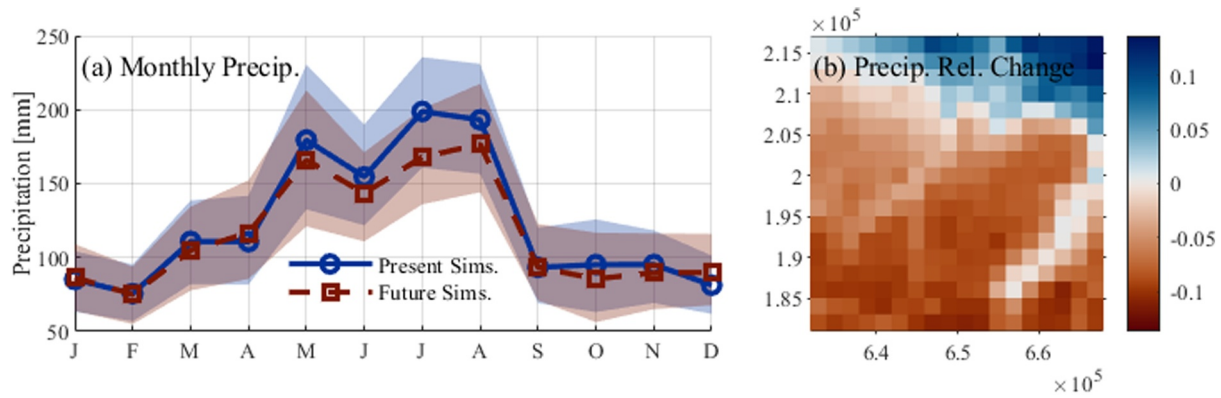


**Figure 7.** Panel (a) shows the mean monthly areal precipitation over the Kleine Emme domain according to the present (blue) and future (red) climate simulations. The shaded areas represent the interquartile range of the means across 900 realizations. The change in total precipitation by the end of the century for each grid cell in the domain is shown in panel (b).

when calculating return periods for extreme precipitation events (Figure 9) following the methodology detailed in Section 4.4.

Consequently, we project a significant increase in hourly precipitation extremes by the end of the century, with the mean change lying within a range of 5%–11% for a broad range of return periods. Conversely, daily precipitation extremes are projected to decrease for lower return periods, with a median value of 9% lower than in the present climate for the 2-year extremes. However, the intensity of less frequent events (e.g., the 200-year return period) is not expected to exhibit any change at the daily scale (a median decrease of 4.1% with IQRs in the order of 16%). These findings contrast glaringly with those derived from the simulations obtained using the previous model. As shown in Moraga et al. (2021), the AWE-GEN-2d simulations projected only minor, statistically insignificant changes to precipitation extremes in the Kleine Emme region for all return periods. This highlights the importance of accounting for the temperature-precipitation dependence and, thus, the influence that the new AWE-GEN-2d-CC formulation has on producing a plausible quantification of climate change impacts on precipitation extremes.

#### 4.7.2. Catchment Response

The increase of hourly precipitation extremes due to accounting for the CC dependence exerts a mild but noticeable influence on streamflow extremes, particularly for rare events. Figure 10a shows this by depicting no change for relatively common hourly peak flows, such as those corresponding to 2 or 5-year return periods, and a

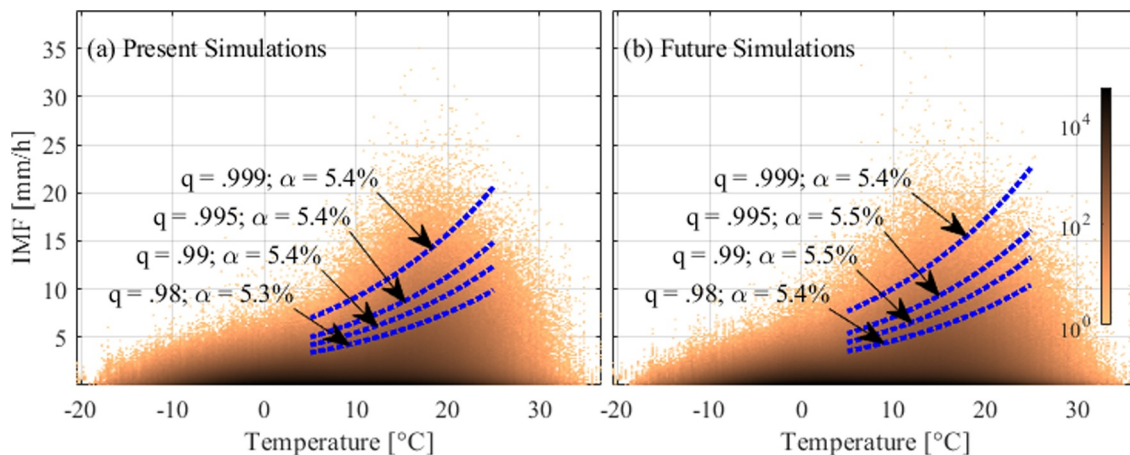


**Figure 8.** Heat maps for the present (left) and future (right) simulated 5-min intensity mean field versus temperature. The colors represent the number of points within each pixel. The quantile regressions for the 98th, 99th, 99.5th, and 99.9th percentiles are superposed as dotted lines. The coefficient  $\alpha$ , included in the labels, denotes the slope of the logarithmic regression for each quantile.

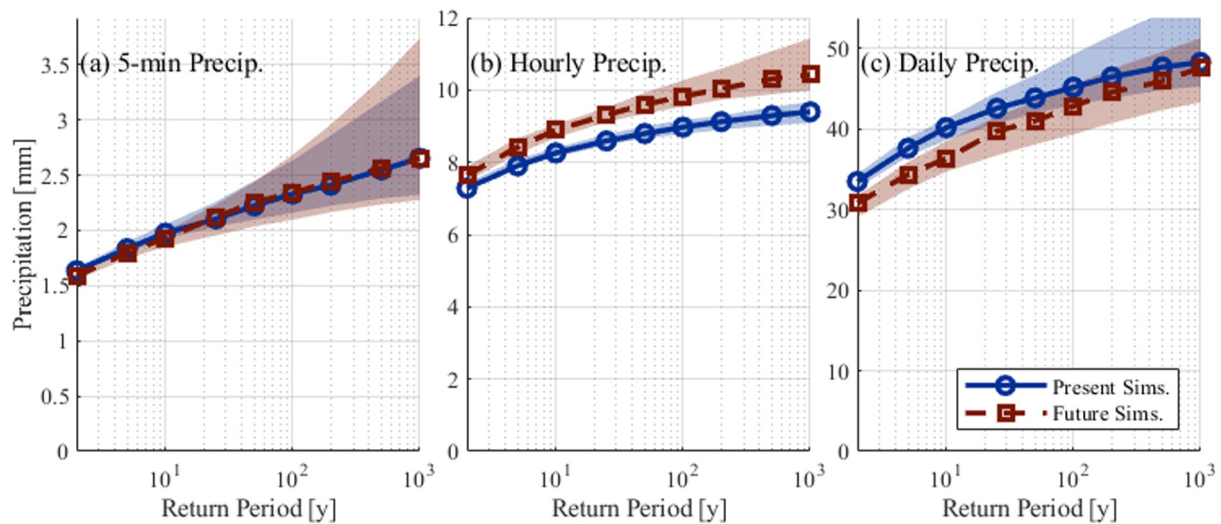


**Figure 9.** Return periods of the 5-min (a), hourly (b), and daily (c) precipitation in present (blue) and future (red) climate conditions. The shaded areas represent the interquartile range.

manifest increase for rarer events, exemplified, for instance, by a 15% rise in the median 50-year return period hourly peak.

Given the distributed nature of the basin response simulation, we can also show how the temperature-precipitation dependence, more pronounced for small-scale convective storm events, is reflected by the magnitude of the peak-flow increase, which looks more pronounced for small-scale basins. This is evident from Figure 10c, where the maximum hourly streamflow exhibits the most dramatic increases for higher elevation and smaller catchments. The improvements due to using the new AWE-GEN-2d-CC model become evident when contrasting the results of these numerical experiments with those obtained using the previous model version. In some instances, the new model chain predicts an over 50% increase for peak flows that exhibited a small decrease in Moraga et al. (2021). Concerning daily extremes, the experiment predicts a decrease ranging from 12% to 15% across return periods, as shown in Figure 10b. This mirrors the projections made using the original AWE-GEN-2d and is explained by the decrease in the intensities of future longer-duration precipitations (Figure 9c) and the increased air temperature that drives drier antecedent conditions for floods (Moraga et al., 2021). In this, our results coincide with other studies showing weak or negative trends in floods over central Europe despite increases in rainfall peaks (Wasko, Nathan, et al., 2021; Wasko, Westra, et al., 2021). Moreover, we explored the impact of climate change on the timing of floods, as illustrated in Figure S11 in Supporting Information S1. The analysis reveals only a minor shift toward earlier occurrence of events, aligning with the weak trends observed for this region by Blöschl et al. (2017).

## 5. Discussion

AWE-GEN-2d-CC marks a step forward in modeling small-scale climate features, particularly over complex terrains. It improves upon AWE-GEN-2d by modeling the characteristics of storms as a temperature-dependent process, therefore implicitly allowing it to reproduce the statistics of high-intensity events that are associated with convective storms. AWE-GEN-2d-CC performs as well or better than its predecessor in reproducing the seasonality, spatial distribution, and marginal distribution of precipitation and temperature, as shown in Section 4.6. Furthermore, AWE-GEN-2d-CC maintains the same level of model parsimony as it requires the same type of data for calibration and does not increase the number of fitted parameters, and AWE-GEN-2d-CC requires the same—rather modest—amount of computational resources as AWE-GEN-2d. For example, a year of simulation for the Kleine Emme domain takes in the order of 15 min using a typical commercial processor.

In our model setup, we consider the temperature-precipitation relationship to be the same for all precipitation events (as shown by Molnar et al. (2015) for this region) instead of an explicit representation of different storm types (e.g., stratiform and convective), mainly because the latter requires identifying storm types from

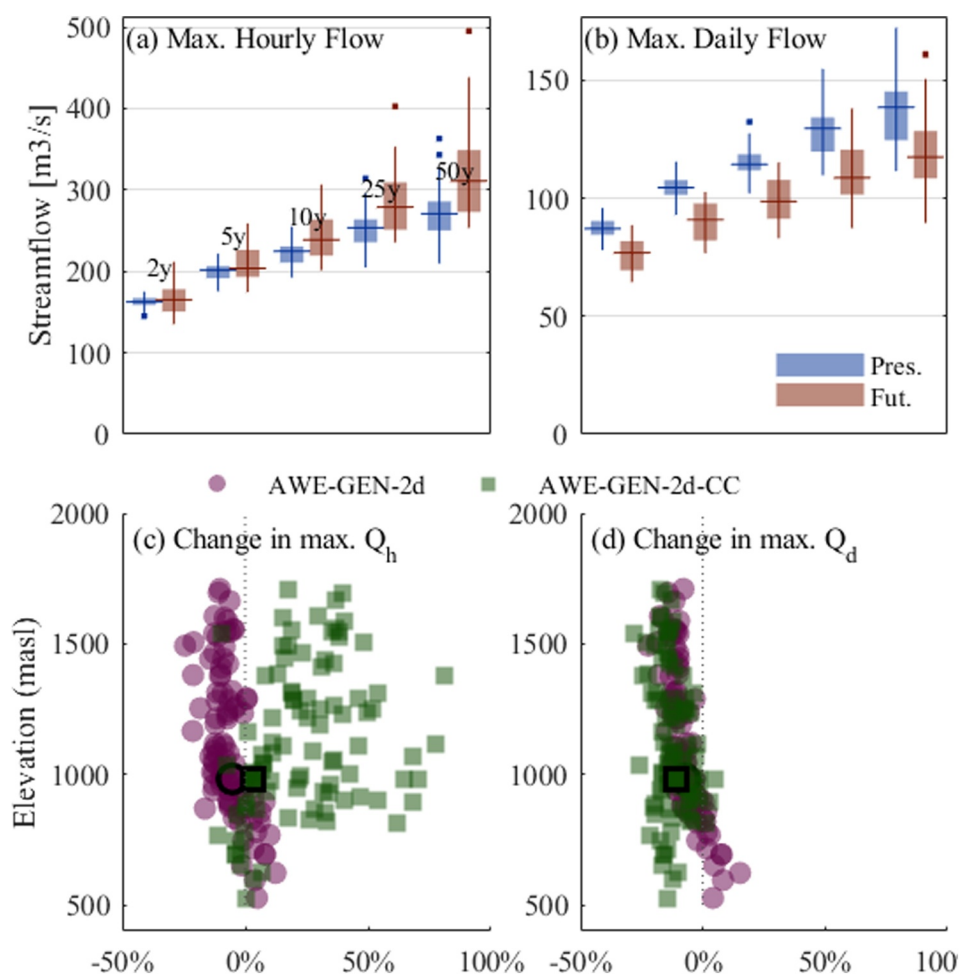


**Figure 10.** The present (blue) and future (red) return periods of maximum hourly and daily streamflow at the outlet of the catchment are shown as boxplots in panels (a) and (b), respectively. Panels (c) and (d) show a comparison of the projected change in the median annual maximum hourly and daily streamflow over the Kleine Emme sub-catchments using the current AWE-GEN-2d-CC model (green squares) and the previous version AWE-GEN-2d (magenta circles).

observational records (Gaál et al., 2014; Jergensen et al., 2020), which, depending on the local climate characteristics, is not straightforward and would add further complexity to the calibration of the WG. As shown in Figure 8, AWE-GEN-2d-CC successfully mimics the observed temperature-precipitation scaling of extreme hourly precipitations. This demonstrates the robustness of the approach to parameterization of the T-P dependence, which, through temperature-bin-dependent calibration, captures the behavior of precipitation extremes in response to temperature variations. It is important to emphasize that the success of the model in emulating the CC scaling relationship arises not from directly imposing of this relationship in the calibration process but from the ability of the model to reproduce observed data patterns. This ensures that the climate projections are grounded in empirically observed relationships, offering a plausible, site-specific and flexible framework for anticipating future climate scenarios.

As demonstrated through the Kleine Emme case study, the temperature scaling feature of the model translates into a predicted intensification in future hourly extremes due to rising temperature (Figure 9). This contrasts with the negligible changes to intensities projected with the previous model formulation (Moraga et al., 2021), and thus demonstrates the value of the new model version. Moreover, studies relying on CPM simulations for central Europe (e.g., Ban et al., 2018; Lenderink et al., 2021) are consistent with the AWE-GEN-2d-CC projections for extreme precipitation. While CPM simulations remain the gold-standard approach to assess small-scale climate change impacts, we argue that comparatively low-cost WGs that can simulate ensembles of credible future climate statistics play a significant role in understanding and adapting to climate change. As such, AWE-GEN-2d-

CC offers a versatile alternative suitable for a myriad of applications in water resource management, agricultural planning, and preparing for natural catastrophes.

It is worth noting that we have limited the scope of this research to the simulation of cloud cover, temperature, and precipitation. However, the satisfactory performance of AWE-GEN-2d-CC in simulating those variables ensures that it can perform as well as AWE-GEN-2d in simulating the remaining climate variables such as relative humidity, atmospheric pressure, incoming short-wave radiation, dew-point temperature, vapor pressure, and near-surface wind speed (Peleg et al., 2017).

Our results also cast light on the future hydrology of the Kleine Emme catchment and how it responds to intensifying extreme precipitations. By the end of the century, rare extreme hourly flows, particularly at higher-elevation sub-catchments, will experience a significant increase (Figure 10). Notably, this is in stark contrast with the results obtained using the previous model, which did not account for temperature scaling in the input precipitation data. For daily extreme flows, however, we project a significant decrease in magnitude explained by the decrease in longer-duration precipitation extremes (Figure 9), and drier antecedent soil conditions (Moraga et al., 2021). In this, our results contradict similar studies carried out for nearby catchments (Brunner et al., 2019; Molnar et al., 2020; Ruiz-Villanueva & Molnar, 2020). We speculate the main sources of discrepancy are related to the treatment of snow-related processes of the respective hydrological models, and the diversity in size and geomorphological properties of the study catchments. In this regard, only replicating this study for a significant number of cases may provide further insight.

## 6. Conclusions

We introduced the AWE-GEN-2d-CC model, a new version of a two-dimensional stochastic WG AWE-GEN-2d-CC (Peleg et al., 2017), which improves upon its predecessor by incorporating the relationship between storm properties and temperature. The improved model was shown to maintain the ability to generate high-resolution gridded climate variables that accurately preserve the auto- and cross-correlations found in the observed records for the Kleine Emme, an exemplary catchment in the Swiss Alps. In particular, the model's performance was evaluated by examining projected climate change impacts on the hydrometeorology of the catchment. AWE-GEN-2d-CC was calibrated using multiple observational and reanalysis data sets, generating a large ensemble (900 years) of present-climate time series. Subsequently, it was re-parameterized to generate downscaled scenarios from nine different GCM-RCM model chains and obtain an equally large ensemble of end-of-the-century climate data.

The ensembles simulated using AWE-GEN-2d-CC successfully replicated the observed temperature scaling of the largest intensities within the 5–25°C temperature range, albeit displaying slightly lower scaling rates. In turn, the simulations yielded an increase in hourly precipitation extremes in the order of 5%–11% by the end of the century, but a decrease in daily precipitation extremes of around 9%. The hydrological response of the Kleine Emme to the changes in precipitation extreme was then examined. It was found that while the high frequency (<5 yr return period) hourly high flows remain at the same level, an increase in the magnitude of hourly high flow rare events (>50 yr return period) was found. Moreover, we found a significant reduction in future daily streamflow extremes.

Our results underscore how the temperature-scaling of storm properties will affect short-duration extreme rainfall events under climate change projections and how it impacts hydrological responses. Consequently, this research highlights the need for a fine-resolution gridded model that accurately simulates the precipitation-temperature relationship, as the AWE-GEN-2d-CC model presented here does. We note that it is essential to model future hydrological extremes utilizing an accurate representation of temperature-induced rainfall intensification, which may extend beyond Alpine catchments, as the one presented here, but may also apply to any fast-responding catchment prone to high-intensity convective storms in general.

## Data Availability Statement

The AWE-GEN-2d-CC model code, as well as an example of the case study presented, is available as a Zenodo repository (Moraga & Peleg, 2023) under a CC BY-NC 4.0 license.

**Acknowledgments**

NP acknowledges the support of the Swiss National Science Foundation (SNSF), Grant 194649.

**References**

Addor, N., Rössler, O., Köplin, N., Huss, M., Weingartner, R., & Seibert, J. (2014). Robust changes and sources of uncertainty in the projected hydrological regimes of Swiss catchments. *Water Resources Research*, *50*(10), 7541–7562. <https://doi.org/10.1002/2014WR015549>

Ali, H., Fowler, H. J., Lenderink, G., Lewis, E., & Pritchard, D. (2021). Consistent large-scale response of hourly extreme precipitation to temperature variation over land. *Geophysical Research Letters*, *48*(4), e2020GL090317. <https://doi.org/10.1029/2020GL090317>

Ali, H., Peleg, N., & Fowler, H. J. (2021). Global scaling of rainfall with Dewpoint temperature reveals considerable Ocean-land difference. *Geophysical Research Letters*, *48*(15), e2021GL093798. <https://doi.org/10.1029/2021GL093798>

Ban, N., Caillaud, C., Coppola, E., Pichelli, E., Sobolowski, S., Adinolfi, M., et al. (2021). The first multi-model ensemble of regional climate simulations at kilometer-scale resolution, Part I: Evaluation of precipitation. *Climate Dynamics*, *2021*(1–2), 1–28. <https://doi.org/10.1007/S00382-021-05708-W>

Ban, N., Rajczak, J., Schmidli, J., & Schär, C. (2018). Analysis of Alpine precipitation extremes using generalized extreme value theory in convection-resolving climate simulations. *Climate Dynamics*, *55*(1–2), 1–15. <https://doi.org/10.1007/s00382-018-4339-4>

Ban, N., Schmidli, J., & Schär, C. (2014). Evaluation of the convection-resolving regional climate modeling approach in decade-long simulations. *Journal of Geophysical Research: Atmospheres*, *119*(13), 7889–7907. <https://doi.org/10.1002/2014JD021478>

Berg, P., Moseley, C., & Haerter, J. O. (2013). Strong increase in convective precipitation in response to higher temperatures. *Nature Geoscience*, *6*(3), 181–185. <https://doi.org/10.1038/ngeo1731>

Blöschl, G., Hall, J., Parajka, J., Perdigão, R. A. P., Merz, B., Arheimer, B., et al. (2017). Changing climate shifts timing of European floods. *Science*, *357*(6351), 588–590. <https://doi.org/10.1126/science.aan2506>

Bordoy, R., & Burlando, P. (2014). Stochastic downscaling of climate model precipitation outputs in orographically complex regions: 2. Downscaling methodology. *Water Resources Research*, *50*(1), 562–579. <https://doi.org/10.1002/wrcr.20443>

Brunner, M. I., Farinotti, D., Zekollari, H., Huss, M., & Zappa, M. (2019). Future shifts in extreme flow regimes in Alpine regions. *Hydrology and Earth System Sciences*, *23*(11), 4471–4489. <https://doi.org/10.5194/hess-23-4471-2019>

Bundesamt für Statistik (BFS). (2020). *Bodeneignungskarte der Schweiz*. Retrieved from <https://dam-api.bfs.admin.ch/hub/api/dam/assets/13147140/master>

Burlando, P., & Rosso, R. (1991). Extreme storm rainfall and climatic change. *Atmospheric Research*, *27*(1), 169–189. [https://doi.org/10.1016/0169-8095\(91\)90017-Q](https://doi.org/10.1016/0169-8095(91)90017-Q)

CH2018. (2019). *CH2018—Climate scenarios for Switzerland, technical report*. National Centre for Climate Services.

Chambers, M. J. (1995). The simulation of random vector time series with given spectrum. *Mathematical and Computer Modelling*, *22*(2), 1–6. [https://doi.org/10.1016/0895-7177\(95\)00106-C](https://doi.org/10.1016/0895-7177(95)00106-C)

Corine Land Cover (CLC). (2014). Corine land cover (CLC) map 2012. Retrieved from <https://land.copernicus.eu/paneurpean/corine-land-cover/clc-2012>

Drobinski, P., Silva, N. D., Panthou, G., Bastin, S., Muller, C., Ahrens, B., et al. (2016). Scaling precipitation extremes with temperature in the mediterranean: Past climate assessment and projection in anthropogenic scenarios. *Climate Dynamics*, *51*(3), 1–21. <https://doi.org/10.1007/s00382-016-3083-x>

Fatichi, S., Ivanov, V. Y., & Caporali, E. (2011). Simulation of future climate scenarios with a weather generator. *Advances in Water Resources*, *34*(4), 448–467. <https://doi.org/10.1016/j.advwatres.2010.12.013>

Fatichi, S., Ivanov, V. Y., Paschalis, A., Peleg, N., Molnar, P., Rimkus, S., et al. (2016). Uncertainty partition challenges the predictability of vital details of climate change. *Earth's Future*, *4*(5), 240–251. <https://doi.org/10.1002/2015EF000336>

Fatichi, S., Peleg, N., Mastrotheodoros, T., Pappas, C., & Manoli, G. (2021). An ecohydrological journey of 4500 years reveals a stable but threatened precipitation–groundwater recharge relation around Jerusalem. *Science Advances*, *7*(37), eabe6303. <https://doi.org/10.1126/sciadv.abe6303>

Fatichi, S., Rimkus, S., Burlando, P., Bordoy, R., & Molnar, P. (2015). High-resolution distributed analysis of climate and anthropogenic changes on the hydrology of an Alpine catchment. *Journal of Hydrology*, *525*, 362–382. <https://doi.org/10.1016/j.jhydrol.2015.03.036>

Fischer, A. M., Keller, D. E., Liniger, M. A., Rajczak, J., Schär, C., & Appenzeller, C. (2015). Projected changes in precipitation intensity and frequency in Switzerland: A multi-model perspective. *International Journal of Climatology*, *35*(11), 3204–3219. <https://doi.org/10.1002/joc.4162>

Fischer, A. M., Strassmann, K. M., Croci-Maspoli, M., Hama, A. M., Knutti, R., Kotlarski, S., et al. (2022). Climate scenarios for Switzerland CH2018—Approach and implications. *Climate Services*, *26*, 100288. <https://doi.org/10.1016/j.cliser.2022.100288>

Fischer, E. M., & Knutti, R. (2016). Observed heavy precipitation increase confirms theory and early models. *Nature Climate Change*, *6*(11), 986–991. <https://doi.org/10.1038/nclimate3110>

Fowler, H. J., Blenkinsop, S., & Tebaldi, C. (2007). Linking climate change modelling to impacts studies: Recent advances in downscaling techniques for hydrological modelling. *International Journal of Climatology*, *27*(12), 1547–1578. <https://doi.org/10.1002/joc.1556>

Fowler, H. J., Lenderink, G., Prein, A. F., Westra, S., Allan, R. P., Ban, N., et al. (2021). Anthropogenic intensification of short-duration rainfall. *Extremes*, *2*(2), 107–122. <https://doi.org/10.1038/s43017-020-00128-6>

Frigo, M., & Johnson, S. G. (1998). FFTW: An adaptive software architecture for the FFT. In *Proceedings of the 1998 IEEE international conference on acoustics, speech and signal processing, ICASSP '98 (Cat. No.98CH36181)* (Vol. 3, pp. 1381–1384). <https://doi.org/10.1109/ICASSP.1998.681704>

Gaál, L., Molnar, P., & Szolgay, J. (2014). Selection of intense rainfall events based on intensity thresholds and lightning data in Switzerland. *Hydrology and Earth System Sciences*, *18*(5), 1561–1573. <https://doi.org/10.5194/hess-18-1561-2014>

Germann, U., Galli, G., Bosacchi, M., & Bolliger, M. (2006). Radar precipitation measurement in a mountainous region. *Quarterly Journal of the Royal Meteorological Society*, *132*(618A), 1669–1692. <https://doi.org/10.1256/qj.05.190>

Gneiting, T., Kleiber, W., & Schlather, M. (2010). Matérn cross-covariance functions for multivariate random fields. *Journal of the American Statistical Association*, *105*(491), 1167–1177. <https://doi.org/10.1198/jasa.2010.tm09420>

Gutowski, W. J., Ullrich, P. A., Hall, A., Leung, L. R., O'Brien, T. A., Patricola, C. M., et al. (2020). The ongoing need for high-resolution regional climate models: Process understanding and stakeholder information. *Bulletin of the American Meteorological Society*, *101*(5), E664–E683. <https://doi.org/10.1175/BAMS-D-19-0113.1>

Jacob, D., Petersen, J., Eggert, B., Alias, A., Christensen, O. B., Bouwer, L. M., et al. (2014). EURO-CORDEX: New high-resolution climate change projections for European impact research. *Regional Environmental Change*, *14*(2), 563–578. <https://doi.org/10.1007/s10113-013-0499-2>

Jenkinson, A. F. (1955). The frequency distribution of the annual maximum (or minimum) values of meteorological elements. *Quarterly Journal of the Royal Meteorological Society*, *81*(348), 158–171. <https://doi.org/10.1002/QJ.49708134804>

- Jergensen, G. E., McGovern, A., Lagerquist, R., & Smith, T. (2020). Classifying convective storms using machine learning. *Weather and Forecasting*, 35(2), 537–559. <https://doi.org/10.1175/WAF-D-19-0170.1>
- Kendon, E. J., Ban, N., Roberts, N. M., Fowler, H. J., Roberts, M. J., Chan, S. C., et al. (2017). Do convection-permitting regional climate models improve projections of future precipitation change? *Bulletin of the American Meteorological Society*, 98(1), 79–93. <https://doi.org/10.1175/BAMS-D-15-0004.1>
- Kotlarski, S., Keuler, K., Christensen, O. B., Colette, A., Déqué, M., Gobiet, A., et al. (2014). Regional climate modeling on European scales: A joint standard evaluation of the EURO-CORDEX RCM ensemble. *Geoscientific Model Development*, 7(4), 1297–1333. <https://doi.org/10.5194/gmd-7-1297-2014>
- Lenderink, G., de Vries, H., Fowler, H. J., Barbero, R., van Uft, B., & van Meijgaard, E. (2021). Scaling and responses of extreme hourly precipitation in three climate experiments with a convection-permitting model. *Philosophical Transactions. Series A, Mathematical, Physical, and Engineering Sciences*, 379(2195), 20190544. <https://doi.org/10.1098/rsta.2019.0544>
- Lochbihler, K., Lenderink, G., & Siebesma, A. P. (2017). The spatial extent of rainfall events and its relation to precipitation scaling. *Geophysical Research Letters*, 44(16), 8629–8636. <https://doi.org/10.1002/2017GL074857>
- Lochbihler, K., Lenderink, G., & Siebesma, A. P. (2019). Response of extreme precipitating cell structures to atmospheric warming. *Journal of Geophysical Research: Atmospheres*, 124(13), 6904–6918. <https://doi.org/10.1029/2018JD029954>
- Lucas-Picher, P., Argüeso, D., Brisson, E., Trambly, Y., Berg, P., Lemonsu, A., et al. (2021). Convection-permitting modeling with regional climate models: Latest developments and next steps. *WIREs Climate Change*, 12(6), e731. <https://doi.org/10.1002/wcc.731>
- Maraun, D., Wetterhall, F., Ireson, A. M., Chandler, R. E., Kendon, E. J., Widmann, M., et al. (2010). Precipitation downscaling under climate change: Recent developments to bridge the gap between dynamical models and the end user. *Reviews of Geophysics*, 48(3), RG3003. <https://doi.org/10.1029/2009RG000314>
- Marra, F., Koukoulou, M., Canale, A., & Peleg, N. (2024). Predicting extreme sub-hourly precipitation intensification based on temperature shifts. *Hydrology and Earth System Sciences*, 28(2), 375–389. <https://doi.org/10.5194/hess-28-375-2024>
- MeteoSwiss. (2016). Daily precipitation (final analysis): RhiresD, Switzerland. Retrieved from <http://www.meteoswiss.admin.ch/home/search.subpage.html/en/data/products/2014/raeumliche-daten-niederschlag.html>
- Molnar, P., Chang, Y. Y., Peleg, N., Moraga, S., Zappa, M., Brunner, M. I., et al. (2020). Future changes in floods. In V. Ruiz-Villanueva & P. Molnar (Eds.), *Past, current, and future changes in floods in Switzerland, Bern, Switzerland: Hydro-CH2018 project* (pp. 51–58). Commissioned by the Federal Office for the Environment (FOEN). <https://doi.org/10.3929/ethz-b-000462778>
- Molnar, P., Faticchi, S., Gaál, L., Szolgay, J., & Burlando, P. (2015). Storm type effects on super Clausius-Clapeyron scaling of intense rainstorm properties with air temperature. *Hydrology and Earth System Sciences*, 19(4), 1753–1766. <https://doi.org/10.5194/hess-19-1753-2015>
- Moraga, J. S., & Peleg, N. (2023). AWE-GEN-2d-CC [Software]. Zenodo. <https://doi.org/10.5281/zenodo.10033795>
- Moraga, J. S., Peleg, N., Faticchi, S., Molnar, P., & Burlando, P. (2021). Revealing the impacts of climate change on mountainous catchments through high-resolution modelling. *Journal of Hydrology*, 603, 126806. <https://doi.org/10.1016/j.jhydrol.2021.126806>
- Moraga, J. S., Peleg, N., Molnar, P., Faticchi, S., & Burlando, P. (2022). Uncertainty in high-resolution hydrological projections: Partitioning the influence of climate models and natural climate variability. *Hydrological Processes*, 36(10), e14695. <https://doi.org/10.1002/hyp.14695>
- Nyman, P., Yeates, P., Langhans, C., Noske, P. J., Peleg, N., Schärer, C., et al. (2021). Probability and consequence of postfire erosion for treatability of water in an unfiltered supply system. *Water Resources Research*, 57(1), 2019WR026185. <https://doi.org/10.1029/2019WR026185>
- O'Donnell, E. C., & Thorne, C. R. (2020). Drivers of future urban flood risk. *Philosophical Transactions of the Royal Society A: Mathematical, Physical & Engineering Sciences*, 378(2168), 20190216. <https://doi.org/10.1098/rsta.2019.0216>
- O'Gorman, P. A., & Schneider, T. (2009). The physical basis for increases in precipitation extremes in simulations of 21st-century climate change. *Proceedings of the National Academy of Sciences*, 106(35), 14773–14777. <https://doi.org/10.1073/pnas.0907610106>
- Paschalis, A., Molnar, P., Faticchi, S., & Burlando, P. (2013). A stochastic model for high-resolution space-time precipitation simulation. *Water Resources Research*, 49(12), 8400–8417. <https://doi.org/10.1002/2013WR014437>
- Peleg, N., Ban, N., Gibson, M. J., Chen, A. S., Paschalis, A., Burlando, P., & Leitião, J. P. (2022). Mapping storm spatial profiles for flood impact assessments. *Advances in Water Resources*, 166, 104258. <https://doi.org/10.1016/j.advwatres.2022.104258>
- Peleg, N., Faticchi, S., Paschalis, A., Molnar, P., & Burlando, P. (2017). An advanced stochastic weather generator for simulating 2-D high-resolution climate variables. *Journal of Advances in Modeling Earth Systems*, 9(3), 1595–1627. <https://doi.org/10.1002/2016MS000854>
- Peleg, N., Marra, F., Faticchi, S., Paschalis, A., Molnar, P., & Burlando, P. (2018). Spatial variability of extreme rainfall at radar subpixel scale. *Journal of Hydrology*, 556, 922–933. <https://doi.org/10.1016/j.jhydrol.2016.05.033>
- Peleg, N., Molnar, P., Burlando, P., & Faticchi, S. (2019). Exploring stochastic climate uncertainty in space and time using a gridded hourly weather generator. *Journal of Hydrology*, 571(3), 627–641. <https://doi.org/10.1016/j.jhydrol.2019.02.010>
- Peleg, N., Sinclair, S., Faticchi, S., & Burlando, P. (2020). Downscaling climate projections over large and data sparse regions: Methodological application in the Zambezi River Basin. *International Journal of Climatology*, 40(15), 6242–6264. <https://doi.org/10.1002/joc.6578>
- Pichelli, E., Coppola, E., Sobolowski, S., Ban, N., Giorgi, F., Stocchi, P., et al. (2021). The first multi-model ensemble of regional climate simulations at kilometer-scale resolution part 2: Historical and future simulations of precipitation. *Climate Dynamics*, 56(11), 3581–3602. <https://doi.org/10.1007/s00382-021-05657-4>
- Prein, A. F., Langhans, W., Fossler, G., Ferrone, A., Ban, N., Goergen, K., et al. (2015). A review on regional convection-permitting climate modeling: Demonstrations, prospects, and challenges. *Reviews of Geophysics*, 53(2), 323–361. <https://doi.org/10.1002/2014RG000475>
- Prein, A. F., Rasmussen, R., Castro, C. L., Dai, A., & Minder, J. (2020). Special issue: Advances in convection-permitting climate modeling. *Climate Dynamics*, 55(1), 1–2. <https://doi.org/10.1007/s00382-020-05240-3>
- Ramirez, J. A., Mertin, M., Peleg, N., Horton, P., Skinner, C., Zimmermann, M., & Keiler, M. (2022). Modelling the long-term geomorphic response to check dam failures in an alpine channel with CAESAR-Lisflood. *International Journal of Sediment Research*, 37(5), 687–700. <https://doi.org/10.1016/j.ijsrc.2022.04.005>
- Rienecker, M. M., Suarez, M. J., Gelaro, R., Todling, R., Bacmeister, J., Liu, E., et al. (2011). MERRA: NASA's modern-era retrospective analysis for research and applications. *Journal of Climate*, 24(14), 3624–3648. <https://doi.org/10.1175/JCLI-D-11-00015.1>
- Ruiz-Villanueva, V., & Molnar, P. (2020). Past, current, and future changes in floods in Switzerland. In V. Ruiz-Villanueva & P. Molnar (Eds.), *Bern, Switzerland: Hydro-CH2018 project. Commissioned by the federal office for the environment (FOEN)*. <https://doi.org/10.3929/ethz-b-000458556>
- Schär, C., Fuhrer, O., Arteaga, A., Ban, N., Charpillou, C., Girolamo, S. D., et al. (2020). Kilometer-scale climate models: Prospects and challenges. *Bulletin of the American Meteorological Society*, 101(5), E567–E587. <https://doi.org/10.1175/BAMS-D-18-0167.1>
- Schirmer, M., Winstral, A., Jonas, T., Burlando, P., & Peleg, N. (2022). Natural climate variability is an important aspect of future projections of snow water resources and rain-on-snow events. *The Cryosphere*, 16(9), 3469–3488. <https://doi.org/10.5194/tc-16-3469-2022>

- Sideris, I. V., Gabella, M., Erdin, R., & Germann, U. (2014). Real-time radar–rain–gauge merging using spatio-temporal co-kriging with external drift in the alpine terrain of Switzerland. *Quarterly Journal of the Royal Meteorological Society*, *140*(680), 1097–1111. <https://doi.org/10.1002/qj.2188>
- Singer, M. B., Michaelides, K., & Hobbey, D. E. J. (2018). STORM 1.0: A simple, flexible, and parsimonious stochastic rainfall generator for simulating climate and climate change. *Geoscientific Model Development*, *11*(9), 3713–3726. <https://doi.org/10.5194/gmd-11-3713-2018>
- Sparks, N. J., Hardwick, S. R., Schmid, M., & Toumi, R. (2018). IMAGE: A multivariate multi-site stochastic weather generator for European weather and climate. *Stochastic Environmental Research and Risk Assessment*, *32*(3), 771–784. <https://doi.org/10.1007/s00477-017-1433-9>
- Steinschneider, S., Ray, P., Rahat, S. H., & Kucharski, J. (2019). A weather-regime-based stochastic weather generator for climate vulnerability assessments of water systems in the western United States. *Water Resources Research*, *55*(8), 6923–6945. <https://doi.org/10.1029/2018WR024446>
- Swisstopo. (2002). *DHM25: Das digitale Höhenmodell der Schweiz*. Bundesamt für Landestopographie.
- Trenberth, K. E., Dai, A., Rasmussen, R. M., & Parsons, D. B. (2003). The changing character of precipitation. *Bulletin of the American Meteorological Society*, *84*(9), 1205–1217. <https://doi.org/10.1175/BAMS-84-9-1205>
- Trzaska, S., & Schnarr, E. (2014). *Methods for climate change impact assessment*. United States Agency for International Development by Tetra Tech ARD.
- Verdin, A., Rajagopalan, B., Kleiber, W., Podestá, G., & Bert, F. (2018). A conditional stochastic weather generator for seasonal to multi-decadal simulations. *Journal of Hydrology*, *556*, 835–846. <https://doi.org/10.1016/j.jhydrol.2015.12.036>
- Vergara-Temprado, J., Ban, N., & Schär, C. (2021). Extreme sub-hourly precipitation intensities scale close to the Clausius-Clapeyron rate over Europe. *Geophysical Research Letters*, *48*(3), e2020GL089506. <https://doi.org/10.1029/2020GL089506>
- Wasko, C., Nathan, R., Stein, L., & O’Shea, D. (2021). Evidence of shorter more extreme rainfalls and increased flood variability under climate change. *Journal of Hydrology*, *603*, 126994. <https://doi.org/10.1016/j.jhydrol.2021.126994>
- Wasko, C., Sharma, A., & Pui, A. (2021). Linking temperature to catastrophe damages from hydrologic and meteorological extremes. *Journal of Hydrology*, *602*, 126731. <https://doi.org/10.1016/j.jhydrol.2021.126731>
- Wasko, C., Sharma, A., & Westra, S. (2016). Reduced spatial extent of extreme storms at higher temperatures. *Geophysical Research Letters*, *43*(8), 4026–4032. <https://doi.org/10.1002/2016GL068509>
- Wasko, C., Westra, S., Nathan, R., Orr, H. G., Villarini, G., Villalobos Herrera, R., & Fowler, H. J. (2021). Incorporating climate change in flood estimation guidance. *Philosophical Transactions. Series A, Mathematical, Physical, and Engineering Sciences*, *379*(2195), 20190548. <https://doi.org/10.1098/rsta.2019.0548>
- Westra, S., Fowler, H. J., Evans, J. P., Alexander, L. V., Berg, P., Johnson, F., et al. (2014). Future changes to the intensity and frequency of short-duration extreme rainfall. *Reviews of Geophysics*, *52*(3), 522–555. <https://doi.org/10.1002/2014RG000464>
- Wilks, D. S., & Wilby, R. L. (1999). The weather generation game: A review of stochastic weather models. *Progress in Physical Geography: Earth and Environment*, *23*(3), 329–357. <https://doi.org/10.1177/030913339902300302>